Journal of Engineering Sciences

Vol 11, Issue 7,July/2020

ISSN NO:0377-9254

PHOTOCATALYTIC DEGRADATION OF SOLOCHROME BLACK UNDER UV LIGHT ON COBALT DOPED TITANIUM DIOXIDE PHOTOCATALYSTS

A M Kalamma[1*], T Subba Rao[1] Ambreensaba Mulla[2], Shirajahammad.M. Hunagund[3], Mohammed Afzal[2]

[1]*Department of Physics, Shri Krishnadevaraya University Ananthapuramu-515003 Andhra Pradesh (AP), India*

[2]*Department of Physics, SECAB's A.R.S.I Degree College for Women, Vijayapur-586101 Karnataka, India*

[3]*Department of physics, SECAB's I.E.T College, Vijayapur-586101 Karnataka, India*

[*]Corresponding Author - email: amkalamma@rediffmail.com

Abstract - In the present investigation well-crystalline cobalt doped TiO_2 nanoparticles (NPs) were prepared by hydrothermal process. The structural, morphological, optical and compositional properties of as prepared samples have been characterized by X-ray diffraction (XRD),field emission scanning electron microscopy (FESEM), UV-Vis spectrophotometry and energy dispersive X-ray spectroscopy (EDS) .XRD analysis reveals that the prepared samples were nanocrystalline and had anatase phase. The average size of crystallites using Scherrer's formula was found to be 7.07nm and 5.73nm for TiO_2 and Co-TiO_2 NPs respectively. FESEM analysis shows the NPs were spherical shape with an average size of about 10nm to 20nm.EDS analysis confirms the chemical compositions of the NPs having Ti and O elements. UV-Vis measurement shows increase in optical band gap due to cobalt doping. The photocatalytic activity was evaluated by monitoring the degradation of Solochrome Black [Eriochrome Black T (EBT)] under UV-light illumination. The photocatalytic degradation results for Solochrome dye were 61.4 % and 78.3 % for TiO_2 NPs and Co-TiO_2 NPs respectively under UV irradiation for 110 minutes. Thus increase in photocatalytic degradation when doped with Co.

Keywords- Hydrothermal synthesis, Photocatalytic degradation, TiO_2 NPs, Co-TiO_2 NPs.

INTRODUCTION

Natural colors is one of the significant gatherings of poisons broadly utilized in material, plastic, medication and numerous different businesses, while the unsafe impacts of natural colors in waste water have been a significant concern and now a significant danger in the earth because of the considerable contamination issues brought about by them. These businesses depleted enormous amount of high substance shading effluents, which are commonly increasingly harmful and impervious to devastation by traditional techniques. An essential basis in the utilization of these colors is that they should be profoundly collected in water and stable in light during washing. The gathering of these colors in the water bodies causes eutrophication, decreases the reoxygenation limit and makes serious harm to the aquatic living beings by impeding the invasion of daylight [1]. They must also be resistant to microbial attack. Therefore, they are not readily degradable and are typically not removed from water by wastewater treatment systems and conventional methods like adsorption, ultra filtration, chemical and electrochemical methods [2]. The predominance of photocatalytic degradation by nanoparticles in wastewater treatment is because of its favourable circumstances over the regular techniques, for example, snappy oxidation, no development of polycyclic items and oxidation of toxins. It is a compelling and quick strategy in the expulsion of contaminations from waste water [3]. In the recent years, numerous metal oxides including TiO_2 [4], ZnO [**5**], and other oxides have attracted growing attentions for photodegradation of organic dyes; TiO_2 is of specific interests because of its ease and high strength. In any case, TiO_2 has been increased momentous consideration as a photocatalyst in corruption of natural poisons. Because of the properties of hostile to oxidation long haul strength, non-harmfulness, solid redox capacity, it has been broadly utilized in the field of photocatality. TiO_2 being a semiconductor with a huge band gap i.e, 3.2, 3.02 and 2.96eV for anatase, rutile and brookite phases individually. As TiO_2 particles, get lighted by photons with vitality more noteworthy than the band width of TiO_2, the valence band electrons will be travelled to the band of conduction which leave gaps in the valence band.

Presently electron gap sets could take an interest into a wide range of substance responses on TiO_2 surface and that at last debases all the toxins in the arrangement. This response prompts recombination of electrons and openings rapidly; in the long run TiO_2's photocatalytic movement incredibly diminishes. To acquire higher photocatalytic action, one usually utilized technique is doping metal and/or non metal particles into the TiO_2's crystal lattice. In photocatalysts, vitality of the episode pillar ought to be equivalent to this boundary that can energize the electron and move to conduction band. By considering the band gap of anatase stage, it is considered as a photocatalyst under UV illumination. As per the examinations, daylight on Earth's surface is around 52 to 55% infrared (over 700 nm), 42 to 43% visible (400 to 700 nm), and 3 to 5% bright (under 400 nm) [6]. Along these lines, planning of photocatalysts with energizing vitality in obvious range or changing the necessary vitality for energizing the electrons can be valuable for utilizing the daylight so as to cleansing of water. While vitality change and capacity is the large test in the modernized world, over these issue is significant for the improvement of synergist and electrochemical innovation [7-10]. Doping is one of the most common methods to change the required energy for exciting of electrons in photocatalysts [11]. Doping can decrease or increase this energy; this change depends on type of photocatalyst and dopants [12]. Vu et al [13-17] incorporating exceptionally dynamic photocatalytic TiO_2 nano tubes by aqueous treatment in the base medium utilizing the commercial powder of TiO_2 as Ti source. In this work, Co was used as dopants in TiO_2 nanostructures and the products were characterized and analysed their photocatalytic solochrome dye degradation under UV light.

2. MATERIALS AND METHODS

2.1 CHEMICALS

Titanium (IV) n butoxide (TNB) wt 99% liquid analytical grade, Cobalt nitrate hexahydrate [Co $(NO_3)_2.6H_2O$] and EDTA (di-sodium salt dehydrate) were purchased from Alfa Aesar Chemicals, India. De-ionized water (DW) was used in the preparation of all solutions.

2.2 SYNTHESIS OF TIO_2 AND CO DOPED TIO_2 NANOPARTICLES

TiO_2 NPs were synthesized using hydrothermal method [18]. 30ml of 0.1M of E.D.T.A ($C_{10}H_{14}N_2Na_2O_8.2H_2O$) was prepared by dispersing 0.56gm of E.D.T.A in 15ml of de-ionised water (DW) with a continuous stirring with the aid of magnetic stirrer for 10 minutes later adding 15ml of DW and 1ml of Titanium (IV) n butoxide was added drop wise with continuous stirring for 30 minutes. The colloidal solution was then transferred to a 50ml Teflon-lined stainless steel auto clave, the autoclave was sealed and placed in an oven at 180^0C for 3hours, then the autoclave was allowed to cool down to room temperature. Under ambient conditions, the reactant mixture was centrifuged to collect the product; the product was washed continuously with DW several times to remove the organic molecules bonded to the surface of the product. The final product was dried in an oven at100^0C for one hour. Same procedure is adopted for Cobalt doped TiO_2 nanoparticles by adding 5ml of 0 .1M [Co $(NO_3)_2.6H_2O$] to the solution, then the prepared sample is used for photodegradation application.

PHOTOCATALYTIC EXPERIMENTS

The photo catalytic reactor is a Pyrex-glass cell with 1.0 L capacity. A 10 W Lamp (Philips) as the UV light source (365 nm) was set in a quartz light holder which immersed in the photo reactor cell. Prior to passing light, the solution was allowed stirred in dark for 60 minutes to accomplish adsorption–desorption balance between the color and photo catalyst. The cell was loaded up with 1mg/L of color arrangement and 1 x 10^{-5} M of the photo catalyst. Magnetic stirrer was used to introduce fresh air bubbles into the suspension using a pump. Dye degradation was inspected by taking 4 mL of the suspension at 10 minutes light time spans. Finally, the rate of degradation was determined from the change in absorbance of Dye solution. Prior to the estimation, the resultant solution was centrifuged for 10min at 5000 rpm to remove any turbidity. Kinetic data were evaluated using Microsoft Excel 2010 program.

2.3 CHARACTERIZATION TECHNIQUES:

2.3.1 UV-VIS SPECTROSCOPY

UV-Vis absorbance spectra in the wavelength range 200-800nm was measured using UV-Vis spectrophotometer (model: SPECORD 200+ Analytikjena)

2.3.2 XRD

The crystal structure of the powder sample at a scanning rate of 0.02^0 per second in the scattering angle range of 20^0 to 80^0 with the use of Cu K_α radiation of wavelength $1.54060A^0$ were analysed by XRD (model: Rigaku pro analytical) Peak analysis was carried out using PCPDFWIN software.

2.3.4 The surface morphology and nano size nature of the samples at an operating voltage 5kV were examined using FE-SEM (model: Xford-EDX system IE 250 X Max 80).

2.3.5 EDS Elemental compositions were analysed using EDS (model: FEI Quanta 200 F).

2.3.6 ZETA POTENTIAL

The zeta potential was based on the surface charge of the particles relative to the local environment of the prepared particle. This electrostatic potential of shear plane of the particle was carried out in ultrasonicated dispersion of 0.01 g/100 mL in DMSO in room temperature using the Horiba SZ-100 nanoparticle analyzer.

3. RESULTS AND DISCUSSIONS

3.1 OPTICAL PROPERTIES:

3.1.1 UV-VIS SPECTROSCOPY;

UV-Vis Spectra were recorded for TiO_2 NPs and Co-TiO_2 NPs in ethanol solvent at room temperature and graphs are shown in Fig 1(a). From the curves it is seen that the absorption maxima (λmax) for TiO_2 NPs and Co-TiO_2 NPs were seen at 341 nm and 370.8 nm separately which is a preliminary indication for the presence of TiO_2 material. The band gap of both the samples were estimated utilizing the absorption information with the assistance of (K–M) transformation method [19].Band gap energy of the semiconductor was estimated using the optical absorption coefficient (α) and is expressed by equation

$$\alpha = \frac{A\left(h\nu - E_g\right)^{1/n}}{h\nu} \qquad (1)$$

Where, hν is energy of photon, E_g is the band gap energy, A is a constant depends on the transition probability and depends on the nature of the transition for allowed direct transition (n= ½), for allowed indirect transition (n=2). In the present cases for an indirect gap, the value of n is 2 for TiO_2 NPs and Co-TiO_2 NPs. Using Tauc's plot the estimated E_g values were found to be 3.07eV and 3.95 eV respectively.

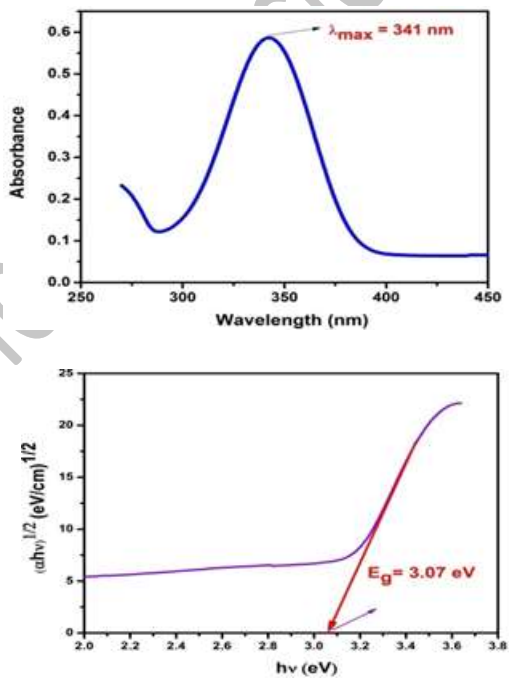

Fig (1) a: UV and Tauc's plot for TiO

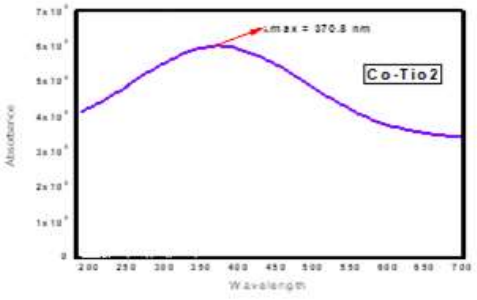

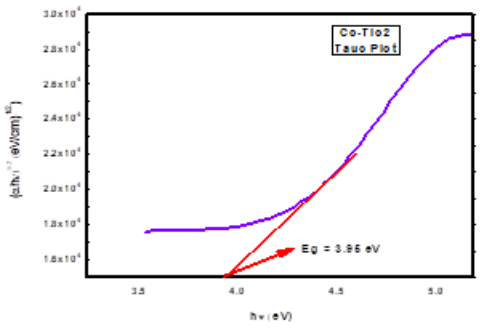

Fig 1(b): UV and Tauc's plot for Co -TiO_2

3.2 STRUCTURAL PROPERTIES:

XRD analysis was carried out to verify the presence of nano crystalline and phase formation. Fig 3 (a and b) shows XRD patterns for TiO_2 and Co-TiO_2 powders respectively it is observed that the presence of strong and sharp peaks; it reveals the formation of the well crystallized samples. From the Fig 3 (a) it is observed that the Bragg's reflection at 2Θ = 25.3429, 37.8769, 47.9727, 54.0791, 62.7467, 75.1348 and 82.6813 can be indexed to (101), (004), (200), (211), (204), (215) and (224) crystal planes respectively. The comparison of 2Θ values in observed Fig 3(a) XRD patterns with those from the standard Joint Committee on Powder Diffraction Standards (JCPDS) data no. 89.4921 confirms the formation of the TiO_2 having anatase phase and tetragonal crystal structure. Fig 3(b) shows the XRD patterns for Co-TiO_2 powders, it is observed that the Bragg's reflection at 2Θ=25.3669, 37.7705, 48.0267, 54.1788, 62.749, 75.1144 and 82.8806 can be indexed to (220), (311), (002), (060), (402), (650) and (660) crystal planes respectively. The comparison of 2Θ values in observed Fig 3(b) XRD patterns with those from the standard Joint Committee On Powder Diffraction Standards (JCPDS) data no. 35.0793 confirms the formation of the Co-TiO_2 having anatase phase and orthorhombic crystal structure. The Scherer's equation [20] is used to estimate an average crystalline size by determining the full width at half maximum (FWHM) of the most intense reflection plane and this equation is given by

$$D \approx \frac{0.9\lambda}{\beta \cos\theta} \qquad (2)$$

Where D is an average crystalline size, λ is the wavelength of X-ray used (1.50406 x 10^{-10} m), Θ is the Bragg's angle in radian and β is the full width at half maximum of the most intense reflection in radian. In our case, the most intense peak for TiO_2 and Co-TiO_2 were found to be (101) and (006) plane and the estimated average crystalline size is 7.07nm and 5.73nm respectively

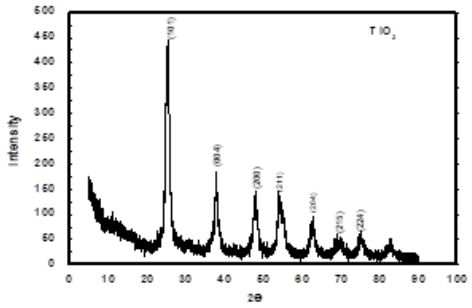

Fig 3 (a) XRD graph for TiO_2

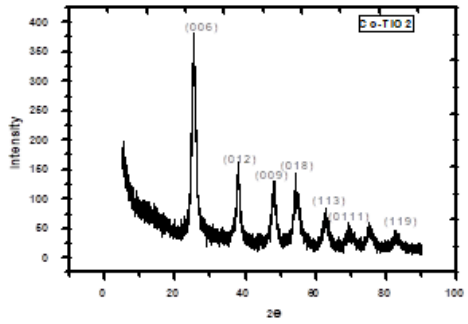

Fig 3 (b) XRD graph for Co-TiO_2

3.3 MORPHOLOGY, SIZE DISTRIBUTION AND ELEMENTAL ANALYSIS

FE-SEM analysis was used to examine the surface morphology and nano size nature of the samples. Fig 4 (a) and Fig 4 (b) shows the particles are having the spherical cluster with average size of about 10 nm to 20 nm. EDS was examined to investigate the chemical composition in $CoTiO_2$ NPs Fig 4 (c) and Fig 4 (d) represents the EDS spectrum for TiO_2 NPs and Co-TiO_2 NPs, hence EDS spectrum confirms the presence of elements i.e. Ti and O, in addition small quantities of element C was observed since it is residue of oil contaminants. The weight percentage (%) and atomic weight percentage (%) Co-TiO_2 NPs are shown inset of Fig 4 (c) and Fig 4 (d)

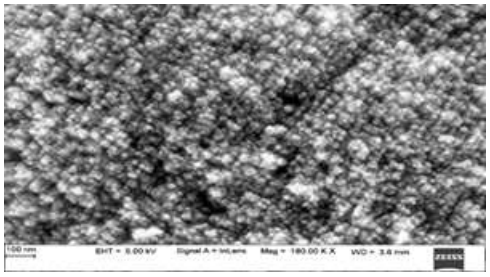

Fig 4(a) FE- SEM image of TiO_2

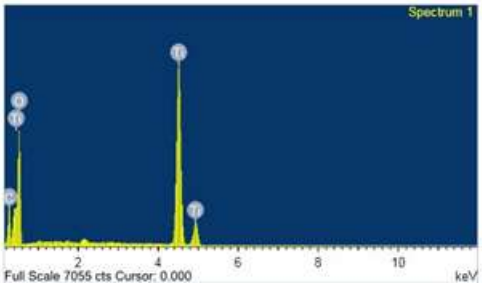

Element	Weight %	Atom %
O k	61.19	55.18
Ti k	57.22	17.23
C k	22.97	27.59

Fig 4(c) EDS spectrum of TiO_2 NPs inset corresponding weight % and atomic % of element

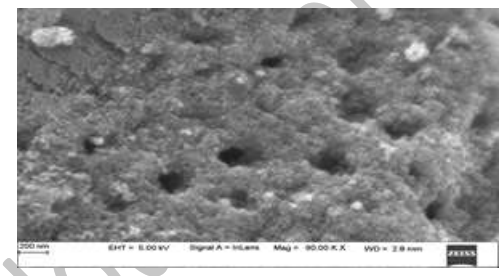

Fig 4(b) FE- SEM image of Co-TiO_2

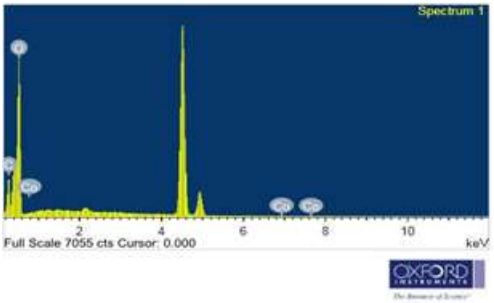

Element	Weight %	Atom %
O	33.77	66.56
Co	0.29	0.16
C	12.68	33.28

Fig 4(d) EDS spectrum of Co-TiO_2 NPs inset corresponding weight % and atomic % of elements

ZETA POTENTIAL STUDY

The zeta potential with a positive value of 30 mV with electrophoretic mobility 0.000061 cm^2/Vs and with positive value of 47.6 mV with electrophoretic mobility 0.000097 cm^2/Vs suspension was obtained for the $TiO_2$and Co-TiO_2 NPs respectively in DMSO and the zeta potential graphs shown in the Fig (5), which clearly shows a stable dispersion without particle settlement. Furthermore, the study of prepared suspension corroborates with general criteria of zeta potential (ζ) value 30 mV with positive or negative sign for better stability.

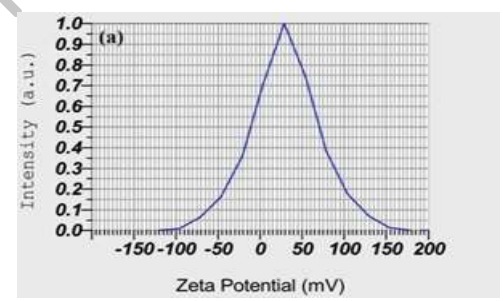

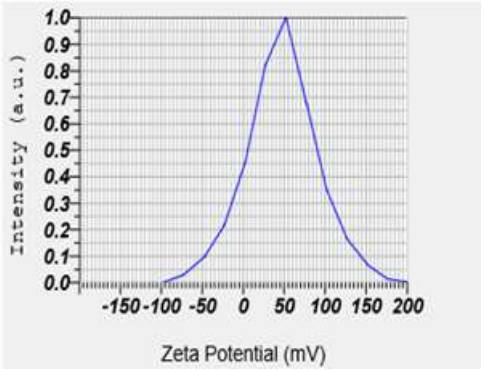

(b)

Fig. 5: Zeta potential evaluation of
(a) TiO_2NPs and (b) Co-TiO_2 NPs in DMSO solvent.

PHOTODEGRADATION PROCESS:

(a)

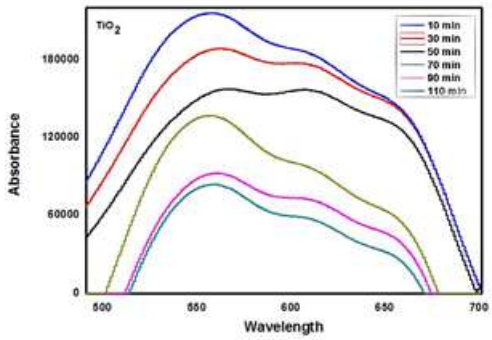

(b)

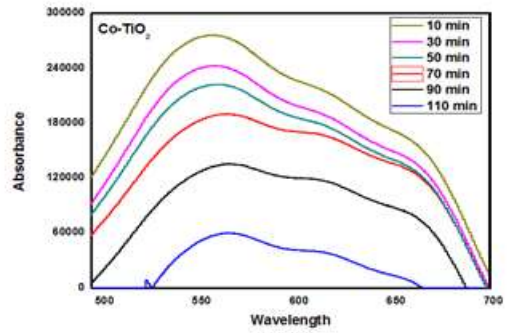

Fig. 6: Photo degradation evaluation of (a) TiO_2 NPs and (b) Co-TiO_2 NPs in solochrome dye solution.

EVALUATION OF PHOTO CATALYTIC ACTIVITY

To assess the photo catalytic activity of TiO_2 NPs, the photo catalytic degradation of solochrome color was performed under UV illumination. The photo catalytic degradation was assessed by estimating the absorbance at customary time stretches. Strikingly, it was seen that the relative absorption intensity constantly diminished as the UV brightening presentation time expanded, altogether demonstrating that solochrome dye degradation viably on the outside of TiO_2 photo catalyst [Fig. 6(a) and Fig 6(b)]. This is on the grounds that, under light, profoundly oxidizing hydroxyl and oxy radicals are shaped by the semiconducting metal oxides like TiO_2, Co-TiO_2 etc. via generation of electron–hole pairs, which break the large organic materials into less harmful small organic materials. The obtained degradation was 61.4 %, 78.3 % within 110 min for TiO_2 and Co-TiO_2 [21].It reveals that after doping with Co percentage of degradation was increased. The Solochrome degradation percentage was calculated as:

$$\text{Degradation rate } (\%) = \frac{A_0 - A}{A_0} \times 10 \quad \textbf{(3)}$$

In order to compare the photo catalytic efficiency of prepared TiO_2 NPs with commercially available photo catalyst such as, TiO_2 & Co-TiO_2 experiments have been done at a fixed solochrome dye concentration for 110 min.

CONCLUSION

Eco friendly hydrothermal route was used for the synthesis of TiO_2 and Co doped TiO_2 nanoparticles and was confirmed by various characterization techniques. The TiO_2 and Co-TiO_2 are having particle size about 10 to 20 nm. Further studied Solochrome dye was degraded under UV light using TiO_2 and Co doped TiO_2 nanoparticles. Among doped TiO_2, the maximum degradation efficiency was found to be 61.4 % for TiO_2 and 78.3 % for Co-TiO_2. From this we can conclude that Co-TiO_2 Shows enhanced photocatalytic activity than bare TiO2.

REFERENCES

[1] Faisal M, Tariq MA, Muneer M (2007) Photocatalysed degradation of two selected dyes in UV-irradiated aqueous suspensions of titania. Dyes Pigm 72: 233–239.

[2] Tang WZ, An H (1995) UV/TiO2 photocatalytic oxidation of commercial dyes in aqueous solutions. Chemosphere 31: 4157–4170.

[3] Sobana N, Muruganadham M, Swaminathan M (2006) Nano-Ag particles doped TiO2 for efficient photodegradation of direct azo dyes. J Mol Catal A 258: 124–132.

[4] El-Kemary M, Abdel-Moneam Y, Madkour M, El-Mehasseb I (2011) Enhanced photocatalytic degradation of Safranin-O by heterogeneous nanoparticles for environmental applications. J Lumin 131: 570-576.

[5] Ullah R, Dutta J (2008) Photocatalytic degradation of organic dyes with manganese-doped ZnO nanoparticles. J Hazard Mater 156: 194-200.

[6] M. Iqbal, An Introduction to Solar Radiation, Elsevier, 2012.

[7] C.M. Magdalane, K. Kaviyarasu, J.J. Vijaya, B. Siddhardha, B. Jeyaraj, Facile synthesis of heterostructured cerium oxide/yttrium oxide nanocomposite in UV light induced photocatalytic degradation and catalytic reduction: synergistic effect of antimicrobial studies, J. Photochem. Photobiol. B Biol. 173 (2017) 23–34.

[8] C.M. Magdalane, K. Kaviyarasu, J.J. Vijaya, C. Jayakumar, M. Maaza, B. Jeyaraj, Photocatalytic degradation effect of malachite green and catalytic hydrogenation by UV–illuminated CeO2/CdO multilayered nanoplatelet arrays: investigation of antifungal and antimicrobial activities, J. Photochem. Photobiol. B Biol. 169 (2017) 110–123.

[9] R. Mendelsberg, J. Kennedy, S. Durbin, R. Reeves, Carbon enhanced blue–violet luminescence in ZnO films grown by pulsed laser deposition, Curr. Appl. Phys. 8 (2008) 283–286.

[10] F.Fang, J. Kennedy,D. Carder,J.Futter, S. Rubanov, Investigations of near infrared reflective behaviour of TiO2 nanopowders synthesized by arcdischarge, Opt. Mater. 36 (2014) 1260–1265.

[11] J.C. Yu, J. Yu, W. Ho, Z. Jiang, L. Zhang, Effects of F-doping on the photocatalytic activity and microstructures of nanocrystalline TiO2 powders, Chem. Mater. 14 (2002) 3808–3816.

[12] A. Zaleska, Doped-TiO2: a review, Recent Patents on Engineering, 2 2008, pp. 157–164.

[13] VU, T.A., DAO, C.D., HOANG, T.T., et al., "Study on photocatalytic activity of TiO2 and non-metal doped TiO2 in Rhodamine B degradation under visible light irradiation", International Journal of Nanotechnology, v. 10, n. 3-4, 235-246, 2013.

[14] ZHENG, S.K., WU, G.H., LIU, L. "First-principles calculations of P-doped anatase TiO2", Acta PhysicaSinica, v. 62, n. 4, pp. 043102, 2013.

[15] YAN, C.Y., YI, W.T., YUAN, H.M., et al., "A highly photoactive S, Cu-codoped nano-TiO2 photocatalyst: Synthesis and characterization for enhanced photocatalytic degradation of neutral red", Environmental Progress & Sustainable Energy, v.33, n. 2, pp. 419-429, 2015.

[16] YI, W.T., YAN, C.Y., YAN, P., et al., "A new perspective for effect of S and Cu on the photocatalytic activity of S, Cu-codoped nano-TiO2 under visible light irradiation", Journal of Sol-Gel Science and Technology, v. 69, n. 2, pp. 386-396, 2014.

[17] WANG, Z., LI, F.F., YANG, C., et al., "Photocatalytic reduction of CO2 using Cu/S-TiO2 prepared by electroless plating method", Advanced Materials Research, v. 233-235, pp. 589-595, 2011.

[18] A M Kalamma[1],T Subba Rao[1],ShirajAhammad Hungund[2], Ambreensaba Mulla[3], Mohammed Afzal[3] "Synthesis and Characterization of Cu And Co Doped TiO_2 Nanoparticles via Hydrothermal Route" JICR ,Volume XII, Issue VI,461, 2020, 0022-1945

[19] ShirajahammadM.Hunagund[a] VaniR.Desai[a] DeliciaA.Barretto[b] MalateshS.Pujar[a] JagadishS.Kadadevarmath[a] ShyamkumarVootla[b] AshokH.Sidarai "Photocatalysis effect of a novel green synthesis gadolinium doped titanium dioxide nanoparticles on their biological activities" Journal of Photochemistry and Photobiology A: Chemistry, 2017, 346, 159-167/

[20] P. B. Patil, V. V. Kondalkar and N. B. Pawar, RSC Adv., 2014, 4, 47278–47286.

[21] UmarfarooqR.Bagwan[a] IrfanN.Shaikh[a] RameshS.Malladi[b] AbdulazizkhanL.Harihar[c] Shirajahammad.M.Hunagund[d] "Effect of titanium dioxide and gadolinium dopants on photocatalytic behavior for acriflavine dye" Journal of Rare Earths, 2020, 38, 234-340.

[22] A. Fujishima and K. Honda // Nature 238 (1972) 37

[23] A. Mills, C. O'Rourke and K. Moore // J. Photoch. Photobio. A **310** (2015) 66.

[24] B. Liu, X. Zhao, C. Terashima, A. Fujishima and K. Nakata // *PCCP* **16** (2014) 8751

[25] C.S. Turchi and D.F. Ollis // J. Catal. **122**(1990) 178

[26] S. Rehman, R. Ullah, A.M. Butt and N.D. Gohar // J. Hazard. Mater. **170** (2009) 560.

[27] Li G, Chen L, Graham M E, et al. A comparison of mixed phase titania photocatalysts prepared by physical and chemical methods: The importance of the solid-solid interface. J Mol Catal A Chem, 2007, 275: 30–35